17th World Conference on Earthquake Engineering, 17WCEE
Sendai, Japan - September 13th to 18th 2020

REAL-TIME HYBRID TESTING OF A PASSIVE VARIABLE ORIFICE DAMPER INCORPORATED INTO BASE ISOLATED BUILDING

K. Ikago[(1)], I. Fukuda[(2)], H. Luo[(3)] , D. Li[(4)], H. Kanno[(5)], N. Hori[(6)]

[(1)] *Professor, International Research Institute of Disaster Science, ikago@irides.tohoku.ac.jp*
[(2)] *Graduate Student, Graduate School of Engineering, Tohoku University, iori.fukuda.q3@dc.tohoku.ac.jp*
[(3)] *PhD Student, Graduate School of Engineering, Tohoku University, luo.hao.q1@dc.tohoku.ac.jp*
[(4)] *Post-doctoral fellow, International Research Institute of Disaster Science, lidaweicc123@163.com*
[(5)] *Associate Professor, Akita Prefectural University, kanno@akita-pu.ac.jp*
[(6)] *Professor, Tohoku Institute of Technology, n-hori@tohtech.ac.jp*

Abstract

In the event of extreme earthquakes in the future such as the expected Nankai megathrust earthquake in Japan and Cascadia earthquake in North America, seismically isolated buildings may undergo excessive displacements beyond their design limit. Indeed, it is reported that the displacement of some residential buildings in Sendai during the Great East Japan Earthquake in 2011 exceeded the design limit of 335 mm, although no severe damage was reported. A simple way of reducing the displacement is to increase the isolator stiffness or the number of damping devices in the isolation layer that may compromise the performance of seismic isolation when subjected to design level earthquakes. Devices that can modify the performance of the isolation system in response to displacement can also be used.

A passive variable orifice damper (PVOD) is an example of a device that can change its damping coefficient and relief force in response to displacement. Unlike a conventional oil damper, a PVOD is equipped with two types of orifices *i.e.* a fixed orifice and a variable orifice valve (VOV). The VOV control is completely passive and no external power source is needed. It has an external hydraulic pilot cylinder that serves as a mechanical displacement detector connected to the VOV. In instances when the displacement detector is not activated, the VOV is open and oil can flow through the two orifices resulting in a low damping coefficient. However, when the displacement results in the prescribed length, the displacement detector is activated and the VOV is closed resulting in an increased damping coefficient that is determined only by the fixed orifice. The relief force of the VOV is proportional to the movement of the displacement detector *i.e.* the difference between the response displacement and the prescribed length.

We successfully developed a prototype PVOD and are currently conducting research on the development of a full-scale damper. The main challenges in developing a full scale PVOD are the manufacturing of the displacement detector and the VOV, although we have experience and know what is needed to manufacture the main part of the PVOD as it is comparable to a regular fluid damper.

We conducted real-time hybrid simulations on a base isolated building equipped with a PVOD where physical specimens of the displacement detector and the VOV were used and the rest of the model including the main part of the damper were a numerical model. The results showed that the mechanical backlash and the air entrained in the hydraulic pilot cylinder had an effect on the performance of the displacement detector.

Keywords: variable orifice damper; extreme earthquake; displacement control design; passive damper

1. Introduction

It is of concern that a seismically isolated building might suffer moat wall impact when subjected to an extreme ground motion beyond design levels. Although increasing the isolator stiffness or the number of damping devices in the isolation layer may be effective in reducing the excessive isolator displacement induced by an extreme ground motion avoiding the moat wall impact, it may compromise the performance of seismic isolation when subjected to design level earthquakes. One of the most straightforward ways to address this issue is to develop an energy dissipating device that can generate its control force in accordance with response displacement. Rate-independent linear damping (RILD) is an ideal mathematical model to represent a damping element that generates resistive force proportional to the displacement and in phase with the velocity. Ikago and Inoue [1] and Luo *et al*. [2] discussed the benefit of RILD in controlling excessive displacement in low-frequency structures. It is interesting that linearizing the modulated homogeneous friction to be implemented by a semi-active device proposed by Inaudi [3] obtains RILD.

This paper aims to examine the feasibility of a full-scale passive variable orifice damper (PVOD). Unlike the other active/semi-active variable orifice dampers developed by many other researchers [4-9], the damping coefficient and the relief force in the PVOD is determined in a totally passive manner [10, 11]. Dehghan *et al*. [10] first developed a passive variable orifice damper (PVOD) and examined its feasibility conducting dynamic testing on a small scaled specimen. However, a full-scale testing on a PVOD yet needs to be performed. The key component of a PVOD is a hydraulic displacement detecting mechanism to be connected to the variable orifice valve (VOV). In this paper, real-time hybrid simulation (RTHS) is conducted on a five-story base-isolated building equipped with a PVOD in which the displacement detecting part is a physical specimen and the rest including the main part of the damper are numerical model. Moreover, the performance of a PVOD is compared with that of a semi-active control.

2. Outline of the Uni-flow type Passive Variable Orifice Damper

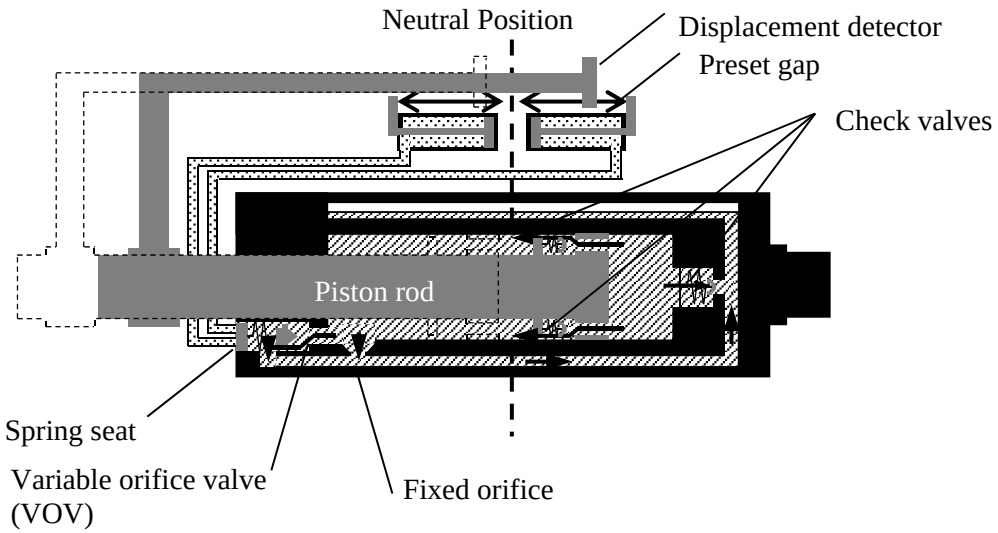

Fig. 1 – Schematic diagram of PVOD

As depicted in Fig. 1 a PVOD has two orifices; a VOV and a fixed orifice. It is a uni-flow type fluid damper; the direction of fluid flow in the orifices is always the same when the piston rod is in both tension and

compression. The piston area of compression side is designed such that it is double of that of tension side to ensure the flow of the fluid is the same in both tension and compression.

Fig. 2 illustrates how the damper parameters change in accordance with the detected displacement. While the hydraulic displacement detector is inactivated, *i.e.*, the piston displacement is less than preset gap L_S, the fluid can flow through the two orifices resulting in a low damping coefficient of C_1. When the displacement of the piston rod exceeds preset gap L_S, the displacement detector is activated to push the spring seat that is connected to the VOV. Then, the VOV is shut resulting in increased damping coefficient of C_2. Once the fluid flows into the VOV, the fluid sent into the VOV flows back to the pilot cylinder very slowly through an adjustable needle valve. Furthermore, when the oil pressure exceeds cracking pressure, the VOV opens and again it results in low damping coefficient of C_1. The relief force F_r is obtaind by the cracking pressure multiplyed by the piston area difference of tension and compression sides. Thus the relief force F_r is determined in accordance with the piston displacment:

$$F_r = \alpha k(x - L_S) \tag{1}$$

where α and k are a coefficient and spring stiffness in the VOV.

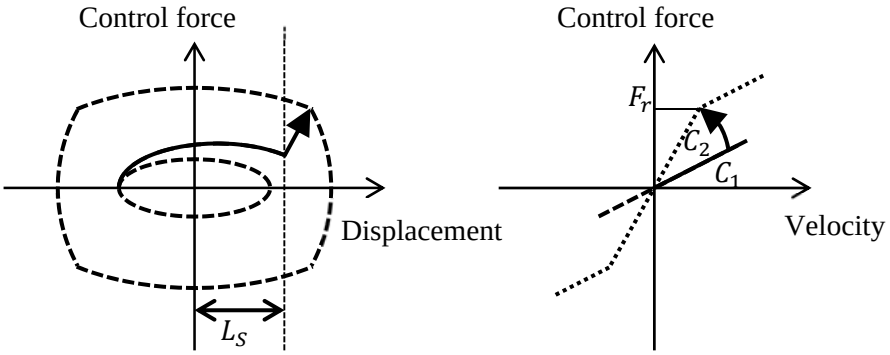

Fig. 2 – Parameter change of PVOD

3. Dynamic Testing on a Partial Specimen of Full-scale PVOD

Dynamic testing is conducted on the key component of a PVOD that consists of a hydraulic displacement detector and VOV (Fig. 3). The gap is set to 50 mm in this testing.

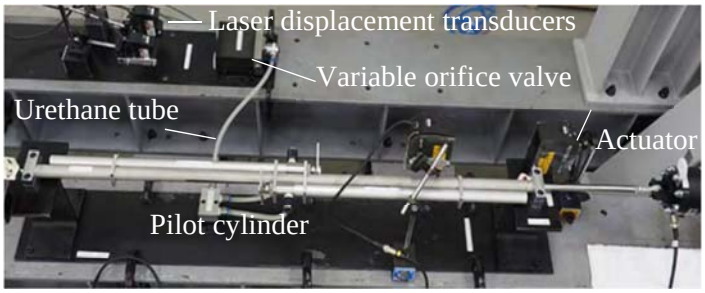

Fig. 3 – Experimental setup

The dynamic testing using a tapered sinusoidal excitation of 0.25Hz confirms that the prototype displacement detecting parts work smoothly as expected. A is applied. As depicted in Fig. 4. the valve seat in the VOV does not move even when the actuator displacement first exceeded the preset gap at around 5 second because of the displacement loss in the device. It first displaces at around 6 second. Further displacement is observed when the absolute maximum actuator displacement is updated at around 8 second. The updated valve seat displacement holds because the adjustable needle valve is completely shut in this experiment. The loss of displacement detected by the pilot cylinder is identified to be 28 mm, which is attributed to the dilation of the urethane tube, the hydraulic spring stiffness, mechanical backlash, the air contained in the oil, and so forth.

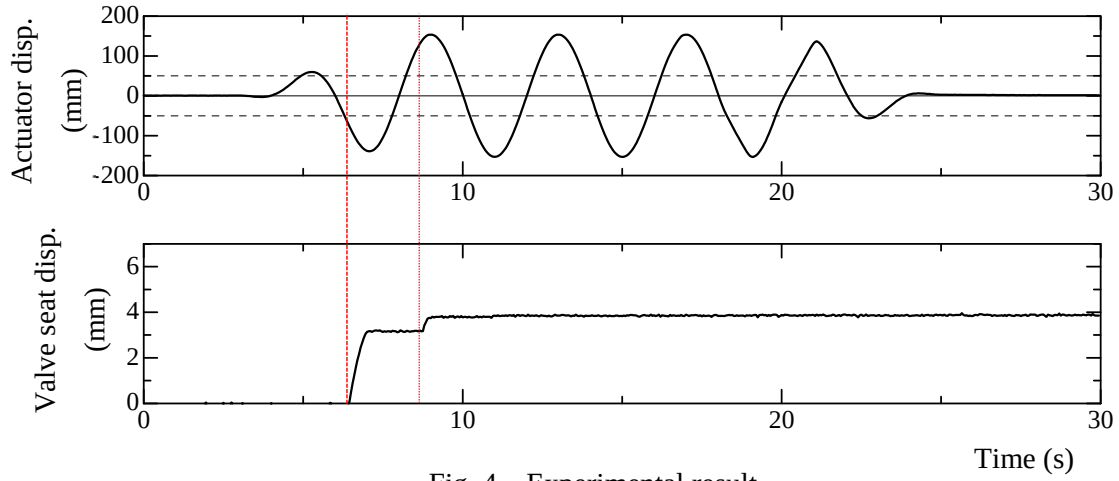

Fig. 4 – Experimental result

4. Real-Time Hybrid Testing

A real-time hybrid testing is conducted on a five story base-isolated building equipped with a PVOD. Because we have experiences in manufacturing fluid dampers having fixed orifices, the testing conducted here focuses on the newly developed VOV that is connected to the hydraulic displacement detector via urethane tubes. Thus, the parts of interest (Fig. 3) are employed as the physical specimen and the rest including the main part of the damper are treated as numerical model.

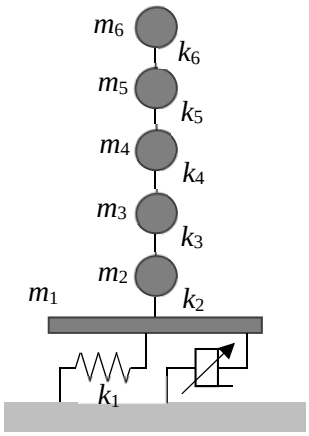

Fig. 5 – Analytical model

Fig. 5 depicts the analytical model and Table 1 summarizes the specification of the building. The fundamental natural period and the damping ratio of the building with the base fixed is 0.67 s and 2% to the critical, respectively. The undamped fundamental natural period when base isolated is 4 s. Four PVODs whose parameters are listed in Table 2 are incorporated into the isolation layer.

Table 1 – Specification of analytical model

Story	Mass (t)	Story stiffness (kN/m)
5	1739	2 290 650
4	1800	2 488 300
3	1807	1 938 750
2	1928	2 037 850
1	2335	1 759 650
Base	3057	31 254
Total	12 666	-

Table 2 – PVOD parameters (per one device)

Damping coefficient	Low (C_1)	784 kNs/m
	High (C_2)	2352 kNs/m
Spring stiffness k		176.4 kN/m
Pilot cylinder	Preset gap	0.05 m
	Maximum stroke	+/- 0.3 m

Table 3 – Ground motion records

Ground motion	Scale factor	Peak ground velocity (m/s)
The 1940 Imperial Valley Earthquake El Centro record NS component	1.0	0.34
The 1968 Tokachi-oki Earthquake Hachinohe harbor record EW component	1.0	0.38
The 1952 Kern County Earthquake Taft record EW component	1.0	0.18
The 1978 Miyagiken-oki Earthquake Tohoku University record NS component	1.0	0.36
The 1995 Kobe Earthquake JMA Kobe record NS component	0.6	0.5

Fig. 6 depicts the comparison of the analytical and hybrid testing results in which the El Centro 1940 NS record is applied. In the testing, the displacement loss in the pilot cylinder that is identified in Section 3 is taken into account. The both results for all the ground motions listed in Table 3 confirmed good agreement.

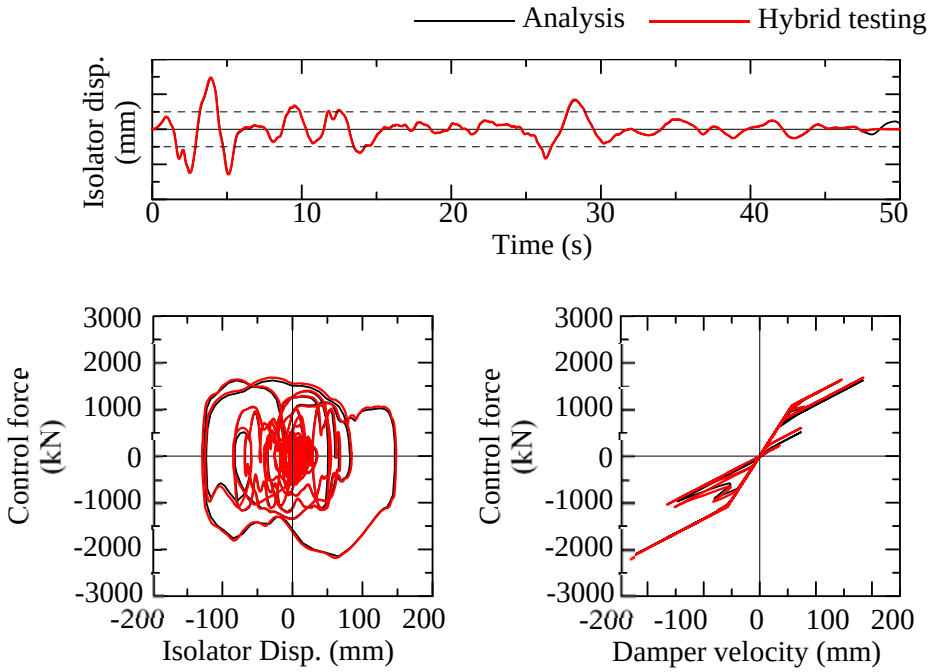

Fig. 6 – Simulation results (El Centro 1940 NS record)

5. Comparison with semi-active strategy

In this section, the performance of an optimally designed PVOD is compared with that of a semi-active damper having the same switchable damping coefficients. Both the passive and semi-active dampers are incorporated in to the same building model used in Section 4. The switchable damping coefficients are the same as those listed in Table 2. For the sake of simplicity, the structure to be controlled is reduced to a single-degree-of-freedom (SDOF) system; the upper structure is regarded as a rigid body because it is relatively stiff compared to the isolators. The suite of ground motions to be applied to the isolation system is the same as that listed in Table 3. The input level of the ground motions are scaled such that the peak ground velocities are 0.25 m/s, 0.5 m/s, and 0.75 m/s, for the moderate design level (Level 1), the severe design level (Level 2), and beyond the design level (Level 3), respectively.

5. 1 Optimum Design of PVOD

Damper parameters of the spring stiffness in the VOV k and the preset gap L_s are taken as the design variable in a multi-objective optimum design of a PVOD to minimize the maximum isolator displacement and control force, in which the other parameters, damping coefficients C_1 and C_2, are fixed to the values listed in Table 2. The optimum designs are sought subject to the following constraints:

1. The maximum isolator displacement is less than 0.5 m to avoid moat wall impact.
2. Base shear coefficient is less than 0.25 when subjected to severe (Level 2) earthquakes.
3. The damping coefficient remain low when subjected to moderate (Level 1) earthquakes.

4. The damping coefficient changes to high damping more than once when subjected to the earthquakes beyond design level.

5. $0 \le k \le 2800$ [kN/m], $0 \le L_S \le 0.4$ [m]

A genetic algorithm is used to find pareto optimal set of designs.

5.2 Sliding Mode Control [12]

We employ a single-degree-of-freedom (SDOF) structure reduced from the building model used in Section 4. Then, the equation of motion for the SDOF model equipped with the semi-active damper is:

$$\dot{X}_s = A_s X_s + B_s F_d + E_s \ddot{x}_0 \tag{2}$$

where,

$$X_s = \begin{Bmatrix} x \\ \dot{x} \end{Bmatrix}, A_s = \begin{bmatrix} 0 & 1 \\ -\dfrac{k}{m} & -\dfrac{c}{m} \end{bmatrix}, B_s = \begin{bmatrix} 0 \\ -\dfrac{1}{m} \end{bmatrix}, E_s = \begin{bmatrix} 0 \\ -1 \end{bmatrix} \tag{3}$$

m, c, and k are the total mass of the structure, the damping coefficient of the isolation layer, and the isolator stiffness, respectively. x and x_0 are the displacement of the mass relative to the ground and the ground displacement, respectively.

Provided that the semi-active damper can be modeled as a Maxwell element as shown in Fig. 7, the derivative of the damping force F_d with respect to the time is expressed as follows:

$$\begin{aligned} \dot{F}_d &= k_d(\dot{x} - \dot{x}_1) \\ &= \frac{k_d}{c_d}(c_d\dot{x} - F_d) \\ &= -\frac{1}{T_d}F_d + \frac{1}{T_d}c_d\dot{x} \end{aligned} \tag{4}$$

where, T_d is the relaxation time.

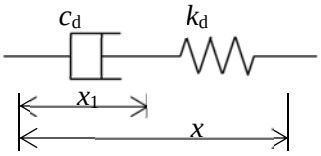

Fig. 7 – Maxwell element

As for the power spectrum of the ground excitation, we employ Kanai-Tajimi spectrum having a fundamental natural frequency of ω_g and a damping ratio of ζ_g for the surface subsoil. Then, the transfer function form the bed rock subjected to the white noise w to the ground surface is obtained by the spectral decomposition of the Kanai-Tajimi filter.

$$\begin{aligned} \dot{Z}_d &= A_d Z_d + D_d w \\ \ddot{x}_0 &= c_d Z_d \end{aligned} \tag{5}$$

where,

$$Z_d = \begin{Bmatrix} x_0 \\ \dot{x}_0 \end{Bmatrix}, A_d = \begin{bmatrix} 0 & 1 \\ -\omega_g^2 & -2\zeta_g\omega_g \end{bmatrix}, D_d = \begin{bmatrix} 0 \\ 1 \end{bmatrix}, C_d = \begin{pmatrix} \omega_g^2 & 2\zeta_g\omega_g \end{pmatrix} \tag{6}$$

Equations for the whole system can be obtained by combining Eqs. (2), (4), and (5).

$$\dot{X}_E = A_E X_E + B_E u + D_E w \tag{7}$$

where,

$$X_E = \begin{Bmatrix} X_S \\ F_d \\ Z_d \end{Bmatrix}, A_E = \begin{bmatrix} A_S & B_S & E_S C_d \\ 0 & -T_d^{-1} & 0 \\ 0 & 0 & A_d \end{bmatrix}, B_E = \begin{bmatrix} 0 \\ T_d^{-1} \\ 0 \end{bmatrix}, u = c_d \dot{x}_1, D_E = \begin{bmatrix} 0 \\ 0 \\ D_d \end{bmatrix} \tag{8}$$

To determine a bilinear optimal control rule S_E that satisfy the condition $J(u_0) = \min_u J(u)$ in the control time segment $[0, T]$, the following performance index is defined:

$$J(u) = E\left[\int_0^T \left[X_E^T Q X_E + u^T R u\right] dt\right] \tag{9}$$

where, the 5×5 matrix Q and the scaler R are the weighting coefficients.

The switching function σ can be obtained from the Hamilton-Jacobi-Bellman equation as follows.

$$\sigma = S_E X_E, S_E = R^{-1} B_E^T P \tag{10}$$

where, P is the solution of the following Riccati Equation.

$$-P = P A_E + A_E^T P - P B_E R^{-1} B_E P + Q,\ P(T) = 0 \tag{11}$$

The control force u_0 can be expressed by the sum of the equivalent control force u_{req} and the control force that compensate the uncertainty u_{nl}.

$$\begin{aligned} u_0 &= u_{req} + u_{nl} \\ u_{req} &= -(S_E B_E)^{-1}(S_E A_E X_E) \\ u_{nl} &= -(S_E B_E)^{-1} K \operatorname{sgn}(\sigma) \end{aligned} \tag{12}$$

where, K is a parameter to ensure the robustness.

Finally, the damping coefficient of the semi-active damper is chosen such that the control force is close to the desired.

$$C_d = \begin{cases} C_1 & \text{if } \dfrac{u_0}{\dot{x}} \le \dfrac{C_1 + C_2}{2} \\ C_2 & \text{if } \dfrac{u_0}{\dot{x}} > \dfrac{C_1 + C_2}{2} \end{cases} \tag{13}$$

Here, two components in the weighting coefficient matrix Q, Q_{11} (a weighting coefficients for isolator displacement) and Q_{33} (a weighting coefficients for control force), are taken as the design variables. A parametric survey is conducted to examine the performance of the semi-active damper.

5.3 Comparison of passive and semi-active control

Fig. 8 compares the performance of the passive and semi-active control when subjected to Level 3 ground motions. In the top left graph, the abscissa and the ordinate represent the maximum isolator displacement and control force, respectively. The red and blue markers show the pareto front for the passive control and the performance of semi-active control, respectively.

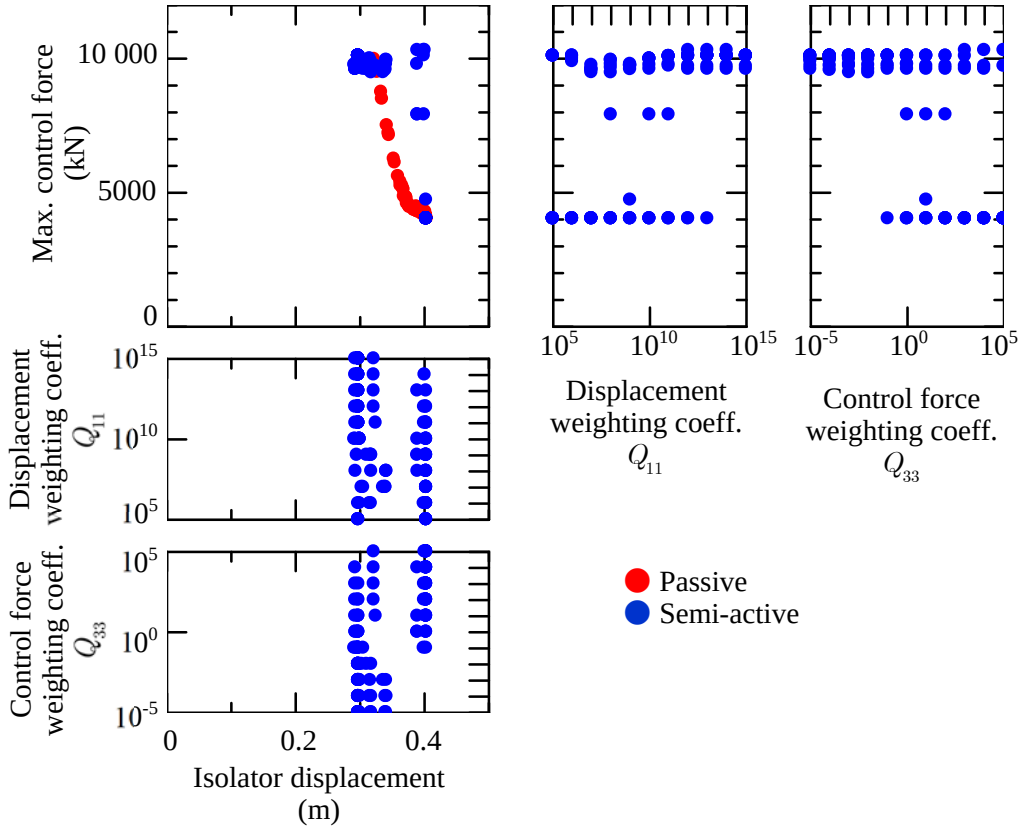

Fig. 8 – Performance comparison on passive and semi-active control

Non-dominated designs can be found for the passive control in the range between 0.3 m and 0.4 m for the isolator displacement. This suggests the possibility of a PVOD to outperform a semi-active control using the same set of damping coefficients. It is observed that the control force increases as the spring stiffness k in the VOV increases resulting in reduction of isolator displacement. On the other hand, the control force decreases as the preset gap L_S increases.

5.3 Conclusions

This paper examined the feasibility of novel passive variable orifice damper (PVOD) by conducting real-time hybrid testing employing the key component of the PVOD, the VOV connected to the hydraulic displacement detector, as the physical specimen. It is confirmed that the VOV worked smoothly as expected. The displacement loss in the hydraulic detector that is attributed to the dilation of the urethane tube, the hydraulic spring stiffness, mechanical backlash, and the air contained in the oil.

Comparison of passive control using PVOD and semi-active damper having the same set of damping coefficients suggests the possibility that passive control using a PVOD can outperform semi-active control.

We are planning to report the dynamic test result of a fully assembled PVOD whose maximum capacity is 500 kN in the near future.

6. References

[1] K. Ikago, N. Inoue (2014): Behavior of Rate-independent Linear Damping Incorporated into Long-period Structures Subjected to Strong Ground Motions. *Proceedings of the 6th World Conference on Structural Control and Monitoring*.

[2] H. Luo, K. Ikago, C. Chong, A. Keivan, B. M. Phillips (2019): Performance of Low-frequency Structures Incorporated with Rate-independent Linear Damping. *Engineering Structures*, 181, 324-335

[3] J. A. Inaudi (1997): Modulated Homogeneous Friction: A Semi-active Damping Strategy. *Earthquake Engineering & Structural Dynamics*, **26**, 361-376.

[4] K. Kawashima, S. Unjoh (1994): Seismic Response Control of Bridges by Variable Dampers. *Journal of Structural Engineering*, ASCE, **120**(9), 2583-2601.

[5] J. N. Yang, J. C. Wu, K. Kawashima, S. Unjoh (1995): Hybrid Control of Seismic-excited Bridge Structures. *Earthquake Engineering & Structural Dynamics*, **24**(11), 1437-1451.

[6] M. D. Symans, M. C. Constantinou (1997): Seismic Testing of a Building Structure with a Semi-active Fluid Damper Control System, Earthquake Engineering and Structural Dynamics, **26**; 759-777.

[7] M. D. Symans, S. W. Kelly (1999): Fuzzy Logic Control of Bridge Structures using Intelligent Semi-active Seismic Isolation Systems, *Earthquake Engineering and Structural Dynamics*, **28**; 37-60.

[8] Z. Liang, M. Tong, G. C. Lee (1995): Real-Time Structural Parameter Modification (RSPM): Development of Innervated Structures, Technical Report NCEER-95-0012.

[9] B. Spencer Jr, S. Nagarajaiah (2003): State of the Art of Structural Control, *Journal of Structural Engineering.* ASCE, **129**(7), 845-856.

[10] S. M. Dehghan B., N. Hori, N. Inoue (2008): Study on Base Isolated Structure with Variable Oil Damper, *Proceedings of the 14th World Conference on Earthquake Engineering*, Paper ID 05-06-0034.

[11] M. Ikenaga, K. Ikago, N. Inoue (2011): Development of a Design Method for Base-isolated Houses with a Variable Oil Damper by an Optimum Design Method, *Proceeding of the 8th International Conference on Structural Dynamics, EURODYN 2011*, Leuven, Belgium, ISBN 978-90-760-1931-4, 1878-1885.

[12] I. Nagashima, Y. Shinozaki, R. Maseki, Y. Sanui, Y. Kitagawa (2010): Sliding Mode Control of Base-Isolation System using Semi-Active Hydraulic Damper. Journal of Structural and Construction Engineering, Architechtural Institute of Japan, **75**(649), 511-519. (in Japanese)

